

The Role of Transmembrane Domain 3 in the Actions of Orthosteric, Allosteric, and Atypical Agonists of the M₄ Muscarinic Acetylcholine Receptor^[S]

Katie Leach, Anna E. Davey, Christian C. Felder, Patrick M. Sexton, and Arthur Christopoulos

Drug Discovery Biology, Monash Institute of Pharmaceutical Sciences and Department of Pharmacology, Monash University, Parkville, Victoria, Australia (K.L., A.E.D., P.M.S., A.C.); and Eli Lilly and Co., Indianapolis, Indiana (C.C.F.)

Received January 2, 2011; accepted February 7, 2011

ABSTRACT

Despite the discovery of a diverse range of novel agonists and allosteric modulators of the M₄ muscarinic acetylcholine (ACh) receptor (mAChR), little is known about how such ligands activate the receptor. We used site-directed mutagenesis of conserved residues in transmembrane 3 (TMIII), a key region involved in G protein-coupled receptor activation, to probe the binding and function of prototypical orthosteric mAChR agonists, allosteric modulators, and “atypical” agonists. We found that most mutations did not affect the binding of the allosteric modulators, with the exception of W108^{3.28}A and L109^{3.29}A (which may contribute directly to the interface between allosteric and orthosteric sites) and mutation D112^{3.32}N (which may cause a global disruption of a hydrogen bond network). Although numerous mutations affected signaling, we did not

identify amino acids that were important for the functional activity of any one class of agonist (orthosteric, allosteric, or atypical) to the exclusion of any others, suggesting that TMIII is key for the transmission of stimulus irrespective of the agonist. We also identified two key residues, Trp108^{3.28} and Asp112^{3.32}, that are essential for the transmission of binding cooperativity between 3-amino-5-chloro-6-methoxy-4-methyl-thieno[2,3-*b*]pyridine-2-carboxylic acid cyclopropylamide (LY2033298) and ACh. Finally, we found that LY2033298 was able to rescue functionally impaired signaling of ACh at the majority of mutants tested in a manner that was inversely correlated with the ACh signaling efficacy, indicating that a key part of the mechanism of the positive cooperativity mediated by LY2033298 on the endogenous agonist involves a global drive of the receptor toward an active conformation.

Introduction

A vast array of ligands, ranging from photons and ions to large glycoproteins, interact with cell-surface GPCRs; these mediate a plethora of physiological functions and comprise one of the largest families of drug targets in the genome (Hopkins and Groom, 2002). Given such importance, an understanding of the structural basis underlying ligand binding and activation of

GPCRs is vital. Although a handful of high-resolution GPCR crystal structures have been solved in recent years, the process remains challenging and the current structures are mostly of inactive state receptors (Lodowski et al., 2009). As a consequence, substantial insights into molecular events governing ligand action at GPCRs continue to be gained through structure-function analyses based on alternative approaches, such as mutagenesis.

The mAChRs are prototypical members of the biogenic amine family A GPCRs, and have long-served as a model system for understanding the structural basis of small-molecule action at these receptors (Hulme et al., 2003). In recent years, there has been a particular resurgence of interest in mechanisms of mAChR activation due to the discovery of novel selective agonists and allosteric modulators of these receptors, especially for the M₁ and M₄ mAChR subtypes (Conn et al., 2009), which represent very attractive targets

This work was supported by the National Health and Medical Research Council (NHMRC) of Australia [Grant 519461]. A.C. is a Senior and P.S. a Principal Research Fellow of the NHMRC.

A.C. is a consultant for Johnson and Johnson and Alchemia. C.C.F. is an employee of Eli Lilly and Co.

Article, publication date, and citation information can be found at <http://molpharm.aspetjournals.org>.
doi:10.1124/mol.111.070938.

[S] The online version of this article (available at <http://molpharm.aspetjournals.org>) contains supplemental material.

ABBREVIATIONS: GPCR, G protein-coupled receptor; ACh, acetylcholine; C₇/3-phth, heptane-1,7-bis-(dimethyl-3'-phthalimidopropyl) ammonium bromide; CHO, Chinese hamster ovary; FBS, fetal bovine serum; LY2033298, 3-amino-5-chloro-6-methoxy-4-methyl-thieno[2,3-*b*]pyridine-2-carboxylic acid cyclopropylamide; mAChR, muscarinic acetylcholine receptor; McN-A-343, 4-*l*-[3-chlorophenyl]carbamoyloxy-2-butynyltrimethylammonium chloride; NDMC, *N*-desmethyloclozapine; [³H]NMS, [³H]*N*-methylscopolamine; [³H]QNB, [³H]quinuclidinyl benzilate; TM, transmembrane domain; ERK1/2, extracellular signal-regulated kinase 1/2; PBS, phosphate-buffered saline; WT, wild type; HA, hemagglutinin.

for the treatment of cognitive deficits associated with diseases such as schizophrenia (Chan et al., 2008; Jones et al., 2008). In contrast to the M₁ mAChR, however, relatively few mutational analyses have been performed on the M₄ mAChR, and thus the structural basis of the subtype-selectivity of novel allosteric modulators and selective agonists is not well established.

The conserved orthosteric site that binds the endogenous agonist, ACh, is located in the top third of the transmembrane helical bundle of the mAChRs and is believed to use contacts provided by inward-facing residues in TM domains III to VII (Hulme et al., 2003). In particular, TMIII contains a number of residues that have been implicated in both the binding and activating mechanisms of the mAChRs by participating in a "global" activation switch that involves a separation of the cytoplasmic region of TMVI away from TMIII and TMVII (Altenbach et al., 1996; Farrens et al., 1996; Gether et al., 1997; Jensen et al., 2001; Hubbell et al., 2003), and movement of the extracellular region of TMVI toward TMIII and TMVII (Elling et al., 1999; Schwartz et al., 2006). Although we recently identified residues in the extracellular portions of the M₄ mAChR that also contribute to ligand-specific activation of the receptor (Nawaratne et al., 2010), the contribution of key TMIII residues in this receptor to the activation mediated by orthosteric and allosteric mAChR ligands remains undetermined.

The current study therefore aimed to provide insight into the role of TMIII on the binding and activation mechanisms used by different classes of M₄ mAChR ligands (Supplementary Fig. 1). These include the prototypical orthosteric agonists, ACh and pilocarpine, the negative allosteric modulator, heptane-1,7-bis-(dimethyl-3'-phthalimidopropyl) ammonium bromide (C₇/3-phth), the novel allosteric agonist and modulator, 3-amino-5-chloro-6-methoxy-4-methyl-thieno[2,3-*b*]pyridine-2-carboxylic acid cyclopropylamide (LY2033298), and the functionally selective agonists, 4-*i*-[3-chlorophenyl]carbamoyloxy-2-butynyltrimethylammonium chloride (McN-A-343) and *N*-desmethyloclozapine (NDMC). Although the basis of the functional selectivity of the latter two compounds remains undetermined, it has been attributed in the past to them interacting with an allosteric site (Sur et al., 2003; May et al., 2007a); in the case of McN-A-343, we have shown that its interaction with the M₂ mAChR, at least, is via a "bitopic" mode that involves concomitant binding to both the orthosteric and an allosteric site (Valant et al., 2008). It is currently unknown whether such a bitopic mechanism is operative at the M₄ mAChR, and thus both McN-A-343 and NDMC are referred to herein as "atypical" agonists. The availability of this diverse repertoire of small-molecule orthosteric, allosteric, and atypical ligands affords, for the first time, an unprecedented opportunity to delineate the role of TMIII in the processes of M₄ mAChR binding, activation, and transmission of cooperativity between two topographically distinct binding domains.

Materials and Methods

Materials. Chinese hamster ovary (CHO) F1pIn cells were from Invitrogen (Carlsbad, CA). Hygromycin B was purchased from Roche Diagnostics (Indianapolis, IN). Dulbecco's modified Eagle's medium and fetal bovine serum (FBS) were from Invitrogen (Carlsbad, CA) and JRH Biosciences (Lenexa, KS), respectively. Primers used for the generation of mutant receptors were purchased from GeneWorks

(Hindmarsh, SA, Australia). The AlphaScreen SureFire phospho-ERK1/2 reagents were kindly donated by Drs. Michael Crouch and Ron Osmond (TGR Biosciences, Thebarton, SA, Australia). AlphaScreen streptavidin donor beads and anti-IgG (protein A) acceptor beads, [³H]quinuclidinyl benzilate ([³H]QNB; specific activity, 52 Ci/mmol), and [³H]*N*-methylscopolamine ([³H]NMS; specific activity, 72 Ci/mmol) were purchased from PerkinElmer Life and Analytical Sciences (Waltham, MA). LY2033298 was synthesized in-house at Eli Lilly (Indianapolis, IN), whereas C₇/3-phth was synthesized in-house by Dr. Celine Valant at the Monash Institute of Pharmaceutical Sciences. All other chemicals were from Sigma-Aldrich (St. Louis, MO).

Receptor Mutagenesis and Generation of Cell Lines. DNA encoding the human M₄ mAChR with a triple HA tag at its amino terminus was purchased from Missouri University of Science and Technology (<http://www.cdna.org>) and cloned into the Gateway destination vector, pEF5/rt/v5/dest, as described previously (Nawaratne et al., 2008). This construct was used to generate M₄ mAChR sequences with the desired amino acid substitutions using QuikChange site-directed mutagenesis (Stratagene, La Jolla, CA) with primers shown in Supplementary Table 1. DNA constructs were transfected into F1pIn CHO cells (Invitrogen) for stable expression according to manufacturer's instructions. Cells were maintained in high-glucose Dulbecco's modified Eagle's medium containing 10% FBS, 16 mM HEPES, and 400 μg/ml hygromycin B.

Radioligand Binding Assays. Cell membranes were prepared as described previously (Nawaratne et al., 2008; Leach et al., 2010). For equilibrium binding, cell membranes (50 μg) were incubated in a final volume of 1 ml of binding buffer [20 mM HEPES, 100 mM NaCl, 10 mM MgCl₂, and 100 μM guanosine-5'-(β-γ-imino)triphosphate, pH 7.4] for 2 h at 37°C with [³H]QNB as described previously (Nawaratne et al., 2008; Leach et al., 2010); [³H]QNB was chosen for the equilibrium binding experiments because it retained appreciable affinity for most of the mutations studied, in contrast to an alternative (and commonly used) prototypical orthosteric antagonist, [³H]NMS. Radioligand dissociation was determined by equilibrating cell membranes (50 μg/1 ml; 1 h, 37°C) with 0.2 nM (wild-type M₄ mAChR) or 1 nM (W108^{3.28}A¹ and L109^{3.29}A) [³H]NMS in binding buffer before the addition of 10 μl of atropine (10 μM) in the absence or presence of modulator using a reverse-time protocol. Receptor-bound radioligand was separated from free radioligand using rapid filtration with a Brandel harvester and radioactivity determined by liquid scintillation counting.

ERK1/2 Phosphorylation Assays. Cells were seeded at 40,000 cells/well into a transparent 96-well plate and grown overnight. Initial time course experiments were used to determine the time required to stimulate maximum ERK1/2 phosphorylation by each agonist, and subsequent concentration-response experiments were conducted by stimulating cells with agonist for 4 min. For interaction studies, in which ACh-stimulated ERK1/2 phosphorylation was measured in the presence of LY2033298, the orthosteric agonist was added to cells immediately after the addition of LY2033298. Phosphorylated ERK1/2 was detected using an AlphaScreen assay as described previously (Nawaratne et al., 2008).

Enzyme-Linked Immunosorbent Assay. Cells were seeded at 75,000 cells/well into a transparent 48-well plate and grown overnight. Cells were washed three times with phosphate-buffered saline (PBS; 137 mM NaCl, 2.7 mM KCl, 4.3 mM Na₂HPO₄, and 1.5 mM KH₂PO₄) and fixed with 4% paraformaldehyde for 15 min at 4°C before two more washes with PBS. Cells were blocked with 5% bovine serum albumin for 45 min and incubated with rabbit anti-HA antibody (Abcam Inc., Cambridge, MA) for 1 h at 37°C. Cells were washed three times with PBS and blocked for a further 15 min with 5% bovine serum albumin. Cells were subsequently incubated with horseradish peroxidase-conjugated anti-rabbit IgG (Cell Signaling

¹ Ballesteros and Weinstein numbers are provided (in superscript) to indicate relative position of residues within the transmembrane domain.

Technology, Danvers, MA) in PBS for 1 h at 37°C before three washes with PBS. The signal was developed using Sigma OPD tablets, and the reaction was stopped by the addition of 3 M HCl. Absorbance was read at 492 nm using an Envision plate reader (PerkinElmer Life and Analytical Sciences).

Data Analysis. Radioligand dissociation kinetic experiments were fitted to a monoexponential decay equation (Motulsky and Christopoulos, 2004), and rate constants determined in the presence of LY2033298 were normalized to those determined in its absence. Competition binding curves between [³H]QNB and unlabeled orthosteric ligands were fitted to a one-site binding model (Motulsky and Christopoulos, 2004). Inhibition experiments that used the allosteric modulators, LY2033298 or C₇/3-phth, were fitted to the following allosteric ternary complex model (Ehlert, 1988):

$$Y = \frac{B_{\max}[A]}{[A] + \left(\frac{K_A K_B}{\alpha' [B] + K_B} \right) \left(1 + \frac{[I]}{K_I} + \frac{[B]}{K_B} + \frac{\alpha [I][B]}{K_I K_B} \right)} \quad (1)$$

where Y is the specific radioligand binding, B_{\max} is the total number of receptors, $[A]$, $[B]$, and $[I]$ are the concentrations of radioligand, allosteric modulator, and unlabeled orthosteric ligand, respectively, K_A , K_B , and K_I are the equilibrium dissociation constants of the radioligand, allosteric modulator, and unlabeled orthosteric ligand, respectively, and α' and α are the cooperativity factors between allosteric modulator and the radioligand or unlabeled orthosteric ligand, respectively. For binding experiments performed with C₇/3-phth versus [³H]QNB, $[I]$ was set to 0 (i.e., no ACh was present in the experiment and the interaction was between C₇/3-phth and [³H]QNB only).

All ERK1/2 phosphorylation assays were analyzed using an operational model of allostereism and agonism according to eq. 2 (Leach et al., 2007, 2010):

$$E = \frac{E_m(\tau_A[A](K_B + \alpha\beta[B]) + \tau_B[B]K_A)^n}{([A]K_B + K_A K_B + [B]K_A + \alpha[A][B])^n + (\tau_A[A](K_B + \alpha\beta[B]) + \tau_B[B]K_A)^n} \quad (2)$$

where E_m is the maximum possible tissue response, $[A]$ and $[B]$ are the concentrations of orthosteric and allosteric ligands, respectively, K_A and K_B are the equilibrium dissociation constant of the orthosteric and allosteric ligands, respectively, τ_A and τ_B are operational measures of orthosteric and allosteric ligand efficacy, respectively, α is the binding cooperativity parameter between the orthosteric and allosteric ligand, and β denotes the allosteric effect of the modulator on the efficacy of the orthosteric agonist. When no allosteric modulator was present, the concentration of $[B]$ was set to 0, and the model becomes identical with the original operational model of agonism described by Black and Leff (1983). Thus, in all instances, agonism is expressed in operational model terms. For the analysis to converge when an allosteric modulator was present, the binding cooperativity with ACh, α , was fixed to that determined separately in radioligand binding assays. In all instances, the equilibrium dissociation constant of each agonist was also fixed to that determined from the binding assays. Finally, to account for effects of the expression level of each of the different mutant receptors on the observed efficacy of each agonist, the B_{\max} values determined from saturation binding were used to normalize the \log_7 values derived from the operational model analysis to what they would be if the mutant were expressed at the same level as the wild-type receptor (Gregory et al., 2010); this corrected efficacy value is denoted as $\log_7 C$.

All affinity, potency, and cooperativity values were estimated as logarithms (Christopoulos, 1998), and statistical comparisons between values for agonists at each different mutant receptor were by one-way analysis of variance using a Dunnett's multiple comparison

post test to determine significant differences between mutant receptors and the wild-type M₄ mAChR. A value of $P < 0.05$ was considered statistically significant.

Results

Rationale for the Choice of Amino Acid Substitutions. A snake diagram of the M₄ mAChR is shown in Fig. 1, highlighting the amino acid residues that were mutated in the current study. We have focused on residues conserved across all five mAChR subtypes located within TMIII because this region is vitally important for both the binding of orthosteric ligands and the activation of the receptor (Hulme et al., 2001, 2003). Very little is known, however, about the role of these residues in the actions of allosteric ligands.

Effects of TMIII Substitutions on the Affinity of Orthosteric and Atypical Ligands. In all assays, the triple HA-tagged wild-type human M₄ mAChR (referred to herein as WT) was compared with the untagged receptor to ensure that the pharmacology of the receptor was not altered by the tag. Although the presence of the HA tag caused a significant reduction in the number of [³H]QNB binding sites detected using saturation binding assays (untagged, 1.35 ± 0.18 pmol/mg protein; HA-tagged, 0.16 ± 0.03 pmol/mg protein; $n = 3-6$), no significant differences were observed between the binding affinity of any of the ligands tested at the tagged and untagged receptor (data not shown). Thus, all subsequent receptor constructs were prepared with the triple HA tag.

As determined by [³H]QNB saturation binding analysis, the exchange of Asp106^{3.26} for alanine or Asp129^{3.49} for asparagine led to a significant reduction in receptor expression compared with the WT, whereas substitution of Val120^{3.40} for alanine resulted in a significant increase in receptor expression levels (Table 1). No [³H]QNB binding was detected after the exchange of Asp112^{3.32} or Tyr113^{3.33} for alanine, although this probably reflects a dramatic inhibitory effect on orthosteric ligand affinity rather than receptor expression because a separate enzyme-linked immunosorbent assay indicated that these latter two constructs were indeed expressed in our FlpIn CHO cells (Supplementary Fig. 2). No other amino acid substitutions had any significant effects on the expression level of the M₄ mAChR (Table 1).

In addition to substitution of Asp112^{3.32} or Tyr113^{3.33} with

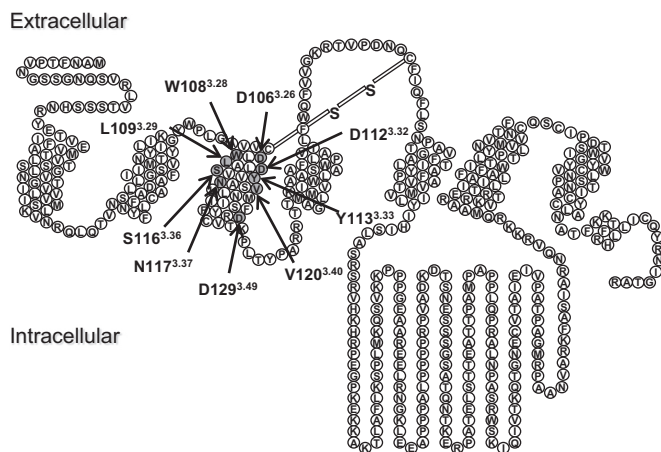


Fig. 1. Snake diagram of the M₄ mAChR. The amino acid residues mutated in this study are highlighted in dark gray.

alanine, substantial effects were noted on ligand affinity for other receptor mutants. In particular, substituting Asp112^{3.32} with asparagine to eliminate the potential ionic interaction with the common ammonium cation of prototypical orthosteric mAChR ligands resulted in a large reduction in the binding affinity of both orthosteric and atypical ligands (Table 1 and Fig. 3). Elongation of the amino acid side chain while retaining the charge of Asp112^{3.32}, by substitution with glutamic acid, had a more selective effect, causing a large reduction in ACh affinity, a modest reduction in pilocarpine affinity, but no effect on the binding of [³H]QNB, McN-A-343, or NDMC (Table 1 and Figs. 2 and 3). A considerable effect on ACh affinity was also observed after substitution of Leu109^{3.29} for alanine, and

smaller effects were observed for other ligands as well (Table 1 and Figs. 2 and 3). Substitution of Ser116^{3.36} or Asn117^{3.37} for alanine had significant inhibitory effects on the binding affinity of ACh but minimal to no effect on the affinity of any of the other ligands. In general, these findings are consistent with the important role these residues play in defining part of the orthosteric pocket for the endogenous agonist. In agreement with recent findings at the M₂ mAChR (Gregory et al., 2010), the W108^{3.28}A mutant M₄ mAChR had opposing effects on ACh affinity (reduction) relative to that of the atypical ligand, NDMC (increase), suggesting that this residue is a key discriminator between the binding poses adopted by these ligands. A different profile was noted upon

TABLE 1
Equilibrium binding parameter estimates for ligands at M₄ mAChR constructs
Values represent the mean ± S.E.M. from at least three separate experiments performed in triplicate. B_{max} is the maximum density of binding sites. pK_A is the negative logarithm of the radioligand equilibrium dissociation constant. pK_B is the negative logarithm of the unlabeled ligand equilibrium dissociation constant.

	[³ H]QNB		pK _B			
	B _{max}	pK _A	ACh	Pilocarpine	NDMC	McN-A-343
	fmol / mg protein					
M ₄ WT	159 ± 28	10.45 ± 0.12	4.89 ± 0.02	5.01 ± 0.13	6.66 ± 0.09	4.92 ± 0.02
M ₄ D106 ^{3.26} A	41 ± 20*	9.70 ± 0.06*	3.95 ± 0.09*	4.24 ± 0.16*	6.67 ± 0.13	4.70 ± 0.14
M ₄ W108 ^{3.28} A	111 ± 21	9.77 ± 0.13*	4.01 ± 0.06*	4.59 ± 0.07	7.08 ± 0.03*	4.88 ± 0.04
M ₄ L109 ^{3.29} A	107 ± 31	9.12 ± 0.10*	3.11 ± 0.09*	4.22 ± 0.11*	5.93 ± 0.02*	4.83 ± 0.17
M ₄ D112 ^{3.32} N	183 ± 12	8.44 ± 0.09*	<2	<3	<4	<3
M ₄ D112 ^{3.32} E	152 ± 39	10.34 ± 0.10	3.19 ± 0.02*	4.16 ± 0.09*	6.52 ± 0.04	4.62 ± 0.02
M ₄ S116 ^{3.36} A	158 ± 18	10.51 ± 0.07	3.61 ± 0.10*	5.09 ± 0.23	6.63 ± 0.02	5.07 ± 0.03
M ₄ N117 ^{3.37} A	260 ± 48	9.95 ± 0.10	3.64 ± 0.04*	4.46 ± 0.04	6.18 ± 0.11*	5.09 ± 0.03
M ₄ V120 ^{3.40} A	264 ± 34*	9.41 ± 0.16*	5.63 ± 0.05*	5.95 ± 0.03*	6.07 ± 0.04*	5.30 ± 0.03
M ₄ D129 ^{3.49} E	77 ± 40	10.14 ± 0.13	5.04 ± 0.07	4.53 ± 0.19	6.69 ± 0.09	4.80 ± 0.15
M ₄ D129 ^{3.49} N	54 ± 9*	10.11 ± 0.17	5.54 ± 0.10*	5.08 ± 0.09	6.57 ± 0.05	5.05 ± 0.08

* p < 0.01, significantly different from WT value as determined by one-way ANOVA with Dunnett's post hoc test.

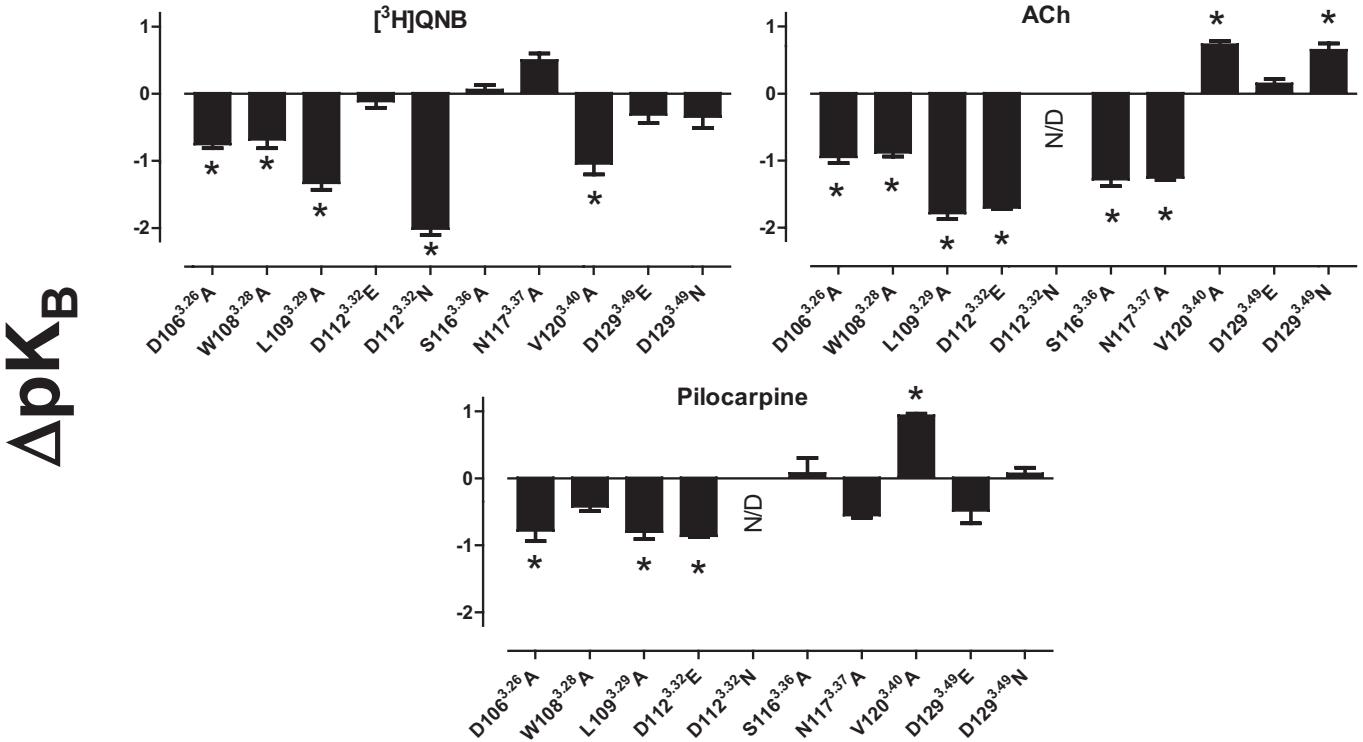


Fig. 2. Mutations in TMIII differentially alter the equilibrium dissociation constant of orthosteric M₄ ligands. Bars represent the change in pK_B of each ligand at the mutant receptor relative to the wild-type receptor, determined from equilibrium radioligand binding assays. Data are mean ± S.E.M. from at least three experiments performed in triplicate. N/D, no detectable binding; *, significant difference to wild type, p < 0.05, one-way analysis of variance, Dunnett's post test.

substitution of Val120^{3,40} for alanine, which caused a modest decrease in the affinity of [³H]QNB and NDMC but a modest increase in the affinity of ACh and pilocarpine. No significant differences were noted in ligand affinities at the D129^{3,49}E mutant, but removal of the charge (D129^{3,49}N) caused a modest increase in ACh affinity.

Effects of TMIII Substitutions on the Affinity of Allosteric Ligands. The interaction between the allosteric modulator C₇/3-phth and the orthosteric antagonist [³H]QNB is characterized by substantial negative cooperativity, and thus, effects of amino acid substitutions on the binding of the modulator could be determined by application of a simple allosteric ternary complex model to the data. In contrast, the interaction

between the allosteric ligand LY2033298 and [³H]QNB is neutrally cooperative (i.e., $\alpha' = 1$; eq. 1) (Nawaratne et al., 2008; Leach et al., 2010), and thus, the effects of receptor mutations on the binding of the latter modulator were determined via an analysis of the interaction between ACh and [³H]QNB in the presence of LY2033298 (Nawaratne et al., 2010).

Perhaps not unexpectedly, the majority of the mutations in TMIII did not have any significant effects on the affinity of the two allosteric modulators (Table 2 and Fig. 3), with a few notable exceptions. Specifically, allosteric ligand affinity was reduced at both the W108^{3,28}A and L109^{3,29}A mutant M₄ mAChRs (Table 2 and Figs. 3 and 4), suggesting that these two residues represent an interface between the prototypical

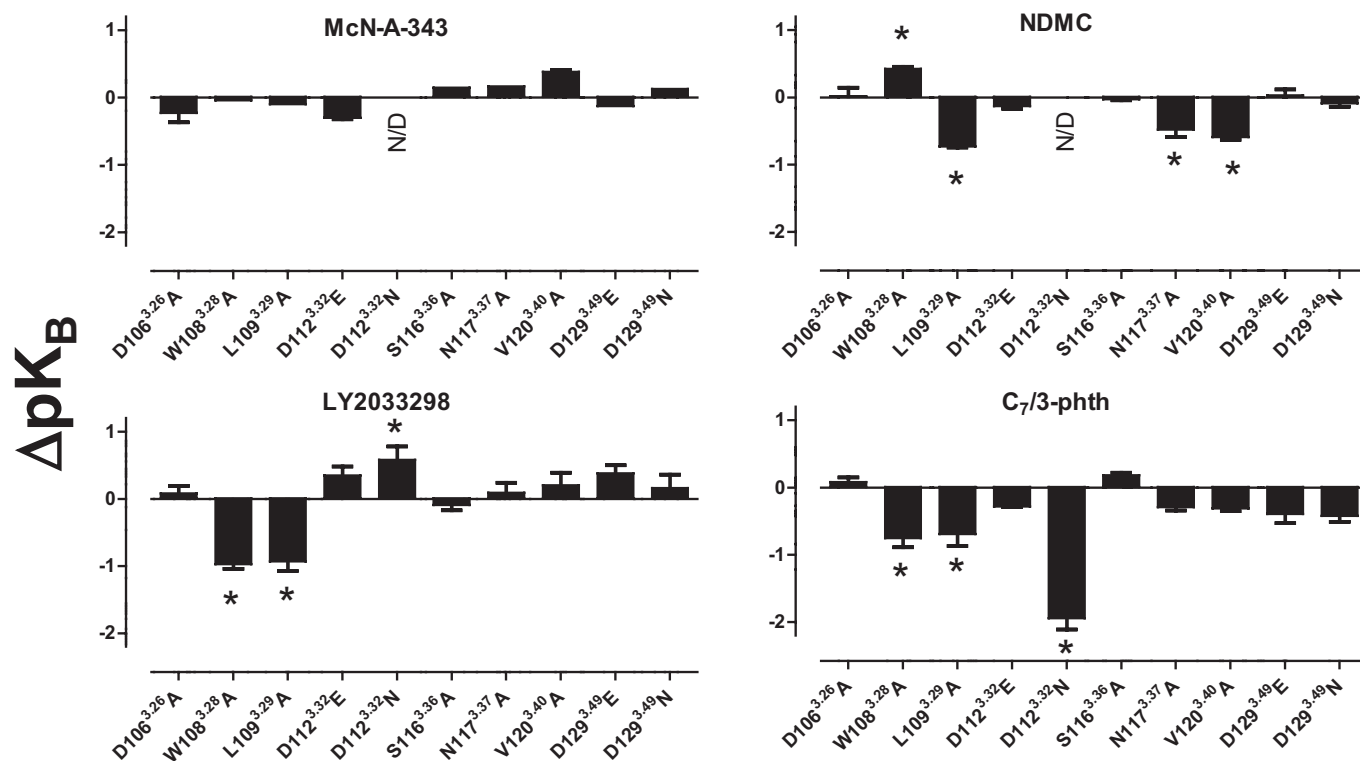


Fig. 3. Mutations in TMIII have differential effects on the equilibrium dissociation constant of allosteric and atypical M₄ ligands. Bars represent the change in pK_B of each ligand at the mutant receptor relative to the wild-type receptor, determined either from equilibrium radioligand binding assays or from nonequilibrium radioligand dissociation assays. Data are mean \pm S.E.M. from at least three experiments performed in triplicate. N/D, no detectable binding; *, significant difference to wild-type, $p < 0.05$, one-way analysis of variance, Dunnett's post test.

TABLE 2

Allosteric modulator equilibrium binding parameters

Values represent the mean \pm S.E.M. from at least three separate experiments performed in triplicate. pK_B is the negative logarithm of the allosteric modulator equilibrium dissociation constant. $\text{Log}\alpha'$ (α') is the logarithm of the cooperativity factor for the interaction between C₇/3-phth and [³H]QNB; antilogarithms are shown in parentheses. $\text{Log}\alpha$ (α) is the logarithm of the cooperativity factor for the interaction between LY2033298 and ACh; antilogarithms are shown in parentheses.

	C ₇ /3-phth		LY2033298	
	pK_B	$\text{Log}\alpha'$ (α')	pK_B	$\text{Log}\alpha$ (α)
M ₄ WT	5.58 \pm 0.03	-1.88 \pm 0.02 (0.01)	5.21 \pm 0.17	1.85 \pm 0.18 (71)
M ₄ D106 ^{3,26} A	5.66 \pm 0.07	-1.19 \pm 0.12* (0.06)	5.29 \pm 0.11	1.51 \pm 0.15 (32)
M ₄ W108 ^{3,28} A	4.83 \pm 0.14*	-1.14 \pm 0.13* (0.07)	4.24 \pm 0.07*	1.23 \pm 0.01* (17)
M ₄ L109 ^{3,29} A	4.89 \pm 0.18*	-1.03 \pm 0.19* (0.09)	4.28 \pm 0.14*	2.54 \pm 0.10* (347)
M ₄ D112 ^{3,32} N	3.64 \pm 0.17*	N.D.	5.79 \pm 0.20*	0.74 \pm 0.08* (5)
M ₄ D112 ^{3,32} E	5.30 \pm 0.01	-1.69 \pm 0.07 (0.02)	5.56 \pm 0.13	0.39 \pm 0.11* (2)
M ₄ S116 ^{3,36} A	5.70 \pm 0.04	-2.09 \pm 0.11 (0.01)	5.12 \pm 0.08	1.54 \pm 0.05 (35)
M ₄ N117 ^{3,37} A	5.29 \pm 0.05	-1.85 \pm 0.14 (0.01)	5.30 \pm 0.15	1.57 \pm 0.13 (37)
M ₄ V120 ^{3,40} A	5.27 \pm 0.04	-1.38 \pm 0.04 (0.04)	5.41 \pm 0.10	1.83 \pm 0.11 (68)
M ₄ D129 ^{3,49} E	5.19 \pm 0.14	-1.51 \pm 0.17 (0.03)	5.59 \pm 0.12	1.61 \pm 0.16 (41)
M ₄ D129 ^{3,49} N	5.16 \pm 0.09	-1.41 \pm 0.08 (0.04)	5.37 \pm 0.20	1.86 \pm 0.22 (72)

N.D., not determined.

* $p < 0.05$, significantly different from WT value as determined by one-way ANOVA with Dunnett's post hoc test.

orthosteric binding site and a more extracellular allosteric site; a previous study of the M_1 mAChR had identified a similar inhibitory effect of the $W^{3.28}A$ on the binding of the allosteric modulator gallamine (Matsui et al., 1995). Because of the indirect nature of the experiments used to determine mutational effects on LY2033298, we also used a second experimental paradigm for determining the potency of this modulator at the two mutants. Specifically, we took advantage of the ability of LY2033298 to allosterically retard the dissociation rate of the orthosteric antagonist [3H]NMS (Leach et al., 2010), which enabled us to measure the LY2033298 concentration range over which this occurred at different receptor constructs (Fig. 5A). Because the cooperativity between LY2033298 and [3H]NMS is also close to neutral at the M_4 mAChR (Leach et al., 2010) (Fig. 5B), the potency (IC_{50}) determined in dissociation kinetic assays will be approximately equal to the K_B value of LY2033298 at the allosteric site (Lazareno and Birdsall, 1995); [3H]NMS was used instead of [3H]QNB for these experiments because the former antagonist has a much faster rate of dissociation than the latter, thus allowing the determination of dissociation kinetics over a reasonable experimental time frame. Accordingly, there was a clear reduction in the potency of LY2033298 to slow [3H]NMS dissociation at both the $W108^{3.28}A$ (pIC_{50} 4.24 ± 0.07 , $n = 3$) and $L109^{3.29}A$ (pIC_{50} 4.28 ± 0.14 , $n = 3$) mutant M_4 mAChRs compared with the WT (pIC_{50} 4.70 ± 0.07 , $n = 3$) (Fig. 5), confirming the results of the equilibrium binding data and indicating that the affinity of LY2033298 for the allosteric site was indeed reduced.

A second surprising finding was that removal of the charge on Asp112^{3.32} through substitution with asparagine had a

profound inhibitory effect on the affinity of $C_7/3$ phth whereas slightly enhancing the affinity of LY2033298 (Table 2, Fig. 3, and Supplementary Fig. 3). Given the important role of this residue as a contact point for ACh and other orthosteric ligands, it is likely that the differential effect of mutation of Asp112^{3.32} on allosteric ligand affinity represents an indirect conformational effect.

Residues in TMIII of the M_4 mAChR Are Involved in Receptor Activation by All Classes of Ligand. We used ERK1/2 phosphorylation as a measure of agonist-stimulated receptor activity because this is a convergent pathway downstream of both G protein-dependent and -independent mechanisms. With the exception of $C_7/3$ -phth, all ligands displayed some agonistic activity at this pathway. We identified a number of residues that contributed to the signaling of orthosteric, allosteric and atypical agonists, as quantified by the operational model $\log\tau_C$ values (Fig. 6 and Table 3). Mutations D106^{3.26}A, L109^{3.29}A, D112^{3.32}E, D112^{3.32}N, S116^{3.36}A, and N117^{3.37}A were detrimental to the efficacy of all agonists tested. We did not identify any residues that contributed solely to the efficacy of one particular class of agonist (e.g., orthosteric, allosteric, or atypical), but substitution of Val120^{3.40} with alanine caused a significant decrease in the efficacy of ACh, LY2033298, and McN-A-343, whereas the efficacy of pilocarpine and NDMC was enhanced by this mutation. Likewise, exchange of Asp129^{3.49} for asparagine had no significant effect on the efficacy of ACh or LY2033298, yet the efficacy of McN-A-343, pilocarpine, and NDMC was increased.

Residues in TMIII Contribute to the Transmission of Cooperativity between the Orthosteric and Allosteric Sites. The ability of an allosteric modulator to alter the function of an orthosteric ligand can be manifested as either

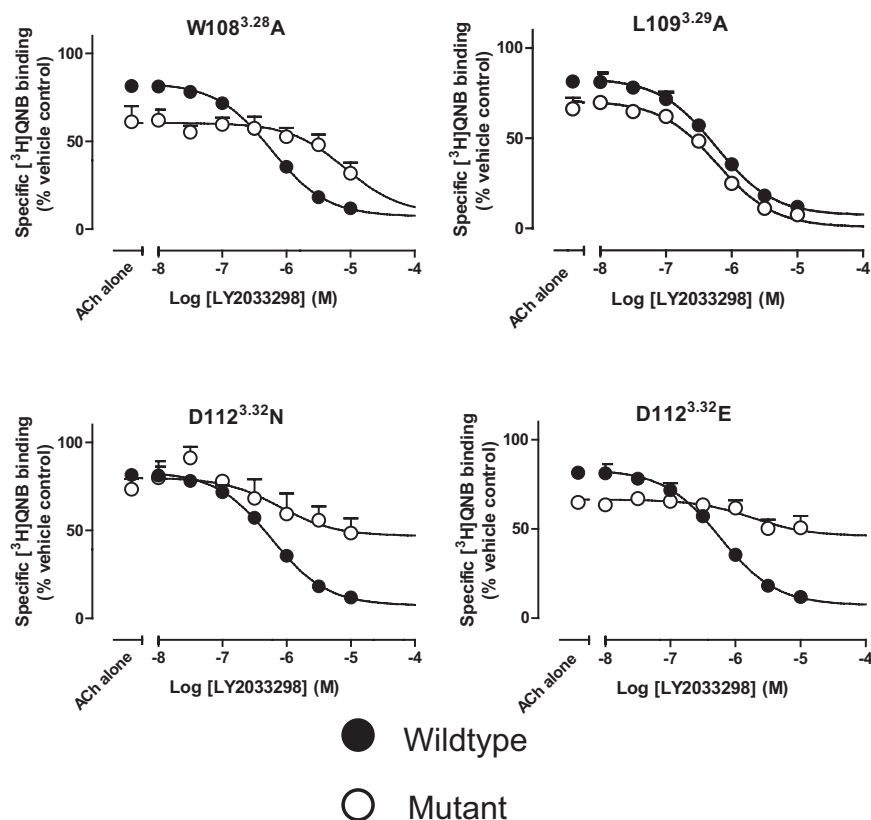


Fig. 4. Radioligand binding interaction studies reveal mutations that alter the cooperativity and/or binding affinity of LY2033298. The competition between a K_A equivalent concentration of [3H]QNB and a fixed concentration of ACh, which inhibited approximately 20% [3H]QNB binding (100 μ M at Trp108^{3.28}, 300 μ M at L109^{3.29}A, 10 mM at D112^{3.32}N, and 1 mM at D112^{3.32}E) was determined in the presence of increasing concentrations of LY2033298 at the indicated mAChR constructs. The curves drawn through the points represent the best global fit of an allosteric ternary complex model (eq. 1) to each pair of datasets (ACh competition of [3H]QNB binding and the IC_{20} concentration of ACh in the presence of LY2033298), with the cooperativity between LY2033298 and [3H]QNB (α') fixed to a value of 1. Data points represent the S.E.M. of at least three experiments performed in triplicate.

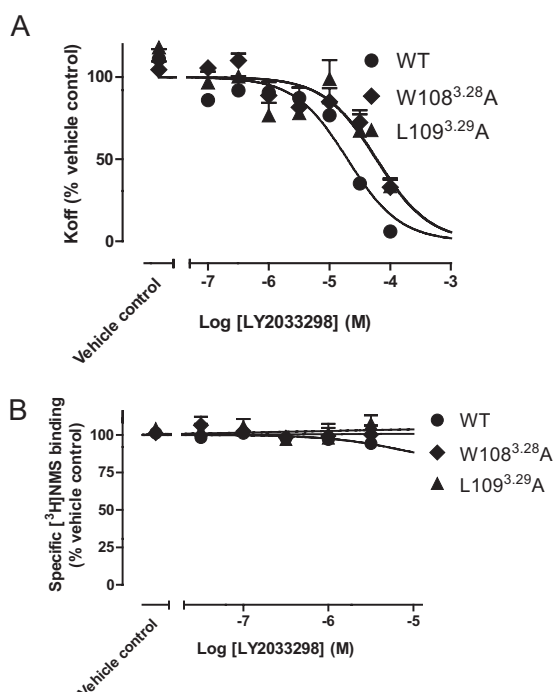


Fig. 5. [³H]NMS dissociation kinetic studies confirm that the W108^{3.28}A and L109^{3.29}A mutations reduce the binding affinity of LY2033298. Concentration-effect relationships for LY2033298 on the dissociation rate (A) or equilibrium binding (B) of [³H]NMS at the wild-type, W108^{3.28}A, or L109^{3.29}A mutants. Data represent mean \pm S.E.M. from three experiments performed in duplicate.

changes in the binding affinity and/or changes in the signaling efficacy of the orthosteric ligand (May et al., 2007b). Thus, we determined the extent to which different amino acid residues in TMIII were involved in the transmission of binding cooperativity (α') between C₇/3-phth and [³H]QNB and both binding cooperativity (α) and efficacy modulation (β) between LY2033298 and ACh; allosteric effects of C₇/3-phth on ACh could not be investigated because of the very high negative cooperativity between this modulator and the agonist (data not shown).

Two mutations, namely W108^{3.28}A and L109^{3.29}A, had substantial effects on the binding cooperativity between each of the modulators and their respective orthosteric interactants (Table 2 and Fig. 4). With regard to W108^{3.28}A, it was of note that both the negative cooperativity between C₇/3-phth and [³H]QNB and the positive cooperativity between LY2033298 and ACh were blunted in each instance (Table 2), suggesting that this residue is not only important for modulator binding affinity but also for the optimal transmission of cooperative effects. In contrast, L109^{3.29}A had opposing effects on cooperativity (i.e., increasing the positive cooperativity between LY2033298 and ACh whereas reducing the negative cooperativity between C₇/3-phth and [³H]QNB). D106^{3.26}A also had a selective (blunting) effect on the negative cooperativity between C₇/3-phth and [³H]QNB. The greatest measurable effect on the binding cooperativity between LY2033298 and ACh was observed at the D112^{3.32}E and D112^{3.32}N mutants, in which a large reduction in the ability of LY2033298 to potentiate ACh binding affinity was observed (Fig. 4 and Table 2). Although the cooperativity between C₇/3-phth and [³H]QNB at the D112^{3.32}N-mutant could not be determined accurately be-

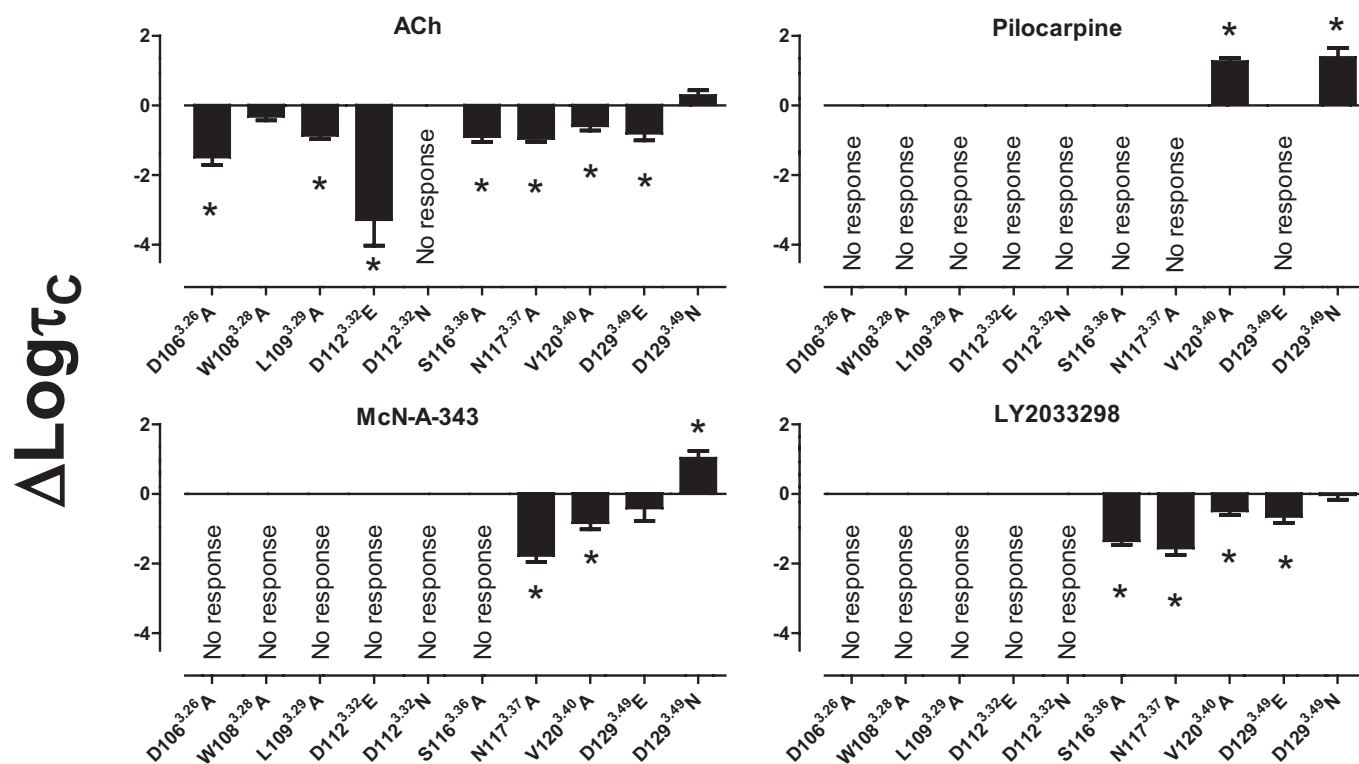


Fig. 6. Agonist efficacy is differentially modified by TMIII mutations. Bars represent the difference in log_{TC} of each agonist, derived from an operational model of agonism (eq. 2), relative to the wild-type receptor value for that agonist. Data represent the mean \pm S.E.M. of at least three experiments performed in triplicate. No response, no detectable response; *, significant difference from the wild-type receptor, $p < 0.05$, one-way analysis of variance, Dunnett's post test.

cause of the pronounced reduction of modulator affinity at this construct (Supplementary Fig. 3), the data were consistent with the retention of substantial negative cooperativity at the mutant because a significant reduction in the binding of [³H]QNB was noted in the presence of high C₇/3-phth concentrations (Supplementary Fig. 3), suggesting that the principal effect of the mutation is on modulator affinity rather than cooperativity.

To determine the effects of amino acid substitutions on the ability of LY2033298 to modulate the signaling efficacy of ACh, we performed functional interaction studies using ERK1/2 phosphorylation as a measure of agonist-mediated receptor activation and fitted the data to an operational model of allosterism and agonism (eq. 2) (Leach et al., 2007, 2010). An internal check of the robustness of the analysis was the excellent correlation between log τ_C estimates obtained for ACh or LY2033298 in experiments when the ligands were tested on their own as agonists (Table 3) compared with when they were coadministered together in the interaction studies (Table 4 and Fig. 7); for the ACh comparison, $r^2 = 0.89$, and for the LY2033298 comparison, $r^2 = 0.95$.

With the exception of the D112^{3.32}A, D112^{3.32}N, and Y113^{3.33}A mutations, in which little or no response was observed to ACh in both the absence or presence of LY2033298, the key finding from the functional interaction experiments was that the allosteric modulator was able to rescue ACh function to varying extents at all other mutant receptors,

with significant increases in the strength of the allosteric modulation of ACh efficacy (β) noted at the L109^{3.29}A, D112^{3.32}E, and S116^{3.36}A mutant receptors (Table 4 and Fig. 7). Indeed, there was a significant inverse correlation ($r^2 = 0.71$) between the observed signaling efficacy of ACh and the ability of LY2033298 to potentiate ACh-mediated signaling, in which lower ACh log τ_C values (more impaired orthosteric agonist signaling) were associated with higher log β values for the interaction (Fig. 8). This finding indicates that a key part of the mechanism of the positive cooperativity mediated by LY2033298 on the endogenous agonist involves a global drive of the receptor toward an active conformation, irrespective of the nature of mutational impairment in TMIII residues.

Discussion

The mAChRs are an important model system for understanding structure-function relationships at family A GPCRs because of the growing number of ligands with novel modes of action being identified for these receptors. In addition to Asp129^{3.49}, located near the cytosolic end of TMIII as part of the highly conserved (E)/DRY activation motif, the current study focused predominantly on amino acid residues that contribute to the top (extracellular-facing) half of TMIII of the M₄ mAChR, which remains less

TABLE 3
Coupling efficiency (log τ_C) parameters of ligands at M₄ mAChR constructs

Values represent the mean \pm S.E.M. from at least three separate experiments performed in triplicate. Log τ_C (τ_C) is the logarithm of the corrected operational efficacy parameter, τ_C , determined via nonlinear regression of the concentration-response data to an operational model of agonism; antilogarithms are shown in parentheses.

	Log τ_C (τ_C)				
	ACh	Pilocarpine	LY2033298	McN-A-343	NDMC
M ₄ WT	2.09 \pm 0.09 (123)	-0.93 \pm 0.08 (0.1)	1.37 \pm 0.08 (23)	0.84 \pm 0.17 (7)	N.R.
M ₄ D106 ^{3.26} A	0.60 \pm 0.22* (4)	N.R.	N.R.	N.R.	N.R.
M ₄ W108 ^{3.28} A	1.77 \pm 0.11 (59)	N.R.	N.R.	N.R.	N.R.
M ₄ L109 ^{3.29} A	1.23 \pm 0.11* (17)	N.R.	N.R.	N.R.	N.R.
M ₄ D112 ^{3.32} N	N.R.	N.R.	N.R.	N.R.	N.R.
M ₄ D112 ^{3.32} E	-1.20 \pm 0.74* (0.06)	N.R.	N.R.	N.R.	N.R.
M ₄ S116 ^{3.36} A	1.19 \pm 0.15* (15)	N.R.	0.02 \pm 0.11* (1)	N.R.	N.R.
M ₄ N117 ^{3.37} A	1.14 \pm 0.09* (14)	N.R.	-0.19 \pm 0.19* (0.7)	-0.93 \pm 0.19* (0.1)	N.R.
M ₄ V120 ^{3.40} A	1.50 \pm 0.13* (32)	0.33 \pm 0.10* (2)	0.88 \pm 0.12* (8)	0.01 \pm 0.19* (1)	-0.85 \pm 0.26 (0.1)
M ₄ D129 ^{3.49} E	1.29 \pm 0.20* (19)	N.R.	0.72 \pm 0.18* (5)	0.43 \pm 0.37 (3)	N.R.
M ₄ D129 ^{3.49} N	2.38 \pm 0.15 (240)	0.45 \pm 0.27* (3)	1.34 \pm 0.14 (22)	1.87 \pm 0.21* (74)	0.19 \pm 0.14 (2)

N.R., no response.
* $p < 0.05$, significantly different from WT value as determined by one-way ANOVA with Dunnett's post hoc test.

TABLE 4
Operational allosteric ternary complex model parameters for the functional interaction between ACh and LY2033298

Parameter values are the mean \pm S.E.M. from at least three experiments performed in triplicate and analyzed according to eq. 2. Log β (β) is the logarithm of the allosteric effect on orthosteric agonist efficacy, β . Log τ_C (τ_C) is the logarithm of the corrected operational efficacy parameter, τ_C .

	Log β (β)	Log τ_C (τ_C)	
		ACh	LY2033298
M ₄ WT	0.90 \pm 0.03 (8)	1.84 \pm 0.12 (69)	1.44 \pm 0.17 (28)
M ₄ D106 ^{3.26} A	0.80 \pm 0.17 (6)	1.24 \pm 0.11 (17)	-1000 ^a
M ₄ W108 ^{3.28} A	1.16 \pm 0.20 (14)	1.49 \pm 0.17 (31)	-1000 ^a
M ₄ L109 ^{3.29} A	1.43 \pm 0.14* (27)	1.17 \pm 0.14 (15)	-1000 ^a
M ₄ D112 ^{3.32} N	N.D.	N.D.	N.D.
M ₄ D112 ^{3.32} E	2.26 \pm 0.16* (182)	-0.80 \pm 0.16* (0.2)	-1000 ^a
M ₄ S116 ^{3.36} A	1.43 \pm 0.14* (27)	0.82 \pm 0.17* (7)	-0.35 \pm 0.45* (0.4)
M ₄ N117 ^{3.37} A	1.27 \pm 0.11 (19)	0.80 \pm 0.27* (6)	-0.27 \pm 0.16* (0.5)
M ₄ V120 ^{3.40} A	0.80 \pm 0.19 (6)	1.47 \pm 0.11 (30)	1.20 \pm 0.19 (16)
M ₄ D129 ^{3.49} E	0.90 \pm 0.09 (8)	1.45 \pm 0.24 (28)	0.78 \pm 0.16 (6)
M ₄ D129 ^{3.49} N	1.04 \pm 0.23 (11)	2.56 \pm 0.39 (363)	1.86 \pm 0.12 (72)

N.D., not determined.
^a log τ_C for LY2033298 was fixed to -1000 (i.e., τ_C approaches 0) as a result of the lack of efficacy of LY2033298.
* $p < 0.05$, significantly different from WT value as determined by one-way ANOVA with Dunnett's post hoc test.

characterized than other mAChR subtypes despite emerging as an exciting drug target for cognitive disorders such as schizophrenia (Chan et al., 2008). The fact that mutations in this region of the receptor had substantial effects on orthosteric, allosteric, and atypical mAChR ligands highlights the pivotal role that TMIII plays in mechanisms of activation and transmission of allosteric effects at the M₄ mAChR. Given the high degree of conservation of these residues across the mAChR and biogenic GPCR families, it is likely that some of the mechanisms inferred from our study will be operative at other GPCRs.

As expected, the majority of TMIII mutations did not substantially affect the binding affinity of the allosteric modulators, C₇/3-phth and LY2033298, with the exception of W108^{3.28}A, L109^{3.29}A, and D112^{3.32}N. Trp108^{3.28} and Leu109^{3.29} are predicted to lie near the junction of TMIII and the extracellular entrance to the orthosteric binding pocket, and it is thus reasonable to hypothesize that these residues

may contribute to lining the “bottom” of a more extracellularly located allosteric binding domain. This hypothesis is also supported by our recent finding that C₇/3-phth and LY2033298 interact in an apparently competitive manner at the M₄ mAChR (Leach et al., 2010), suggesting that they share overlapping binding regions on the receptor. The effect of removing the charge on Asp112^{3.32} was unexpected because of the fact that this residue is the key counter ion that interacts with the ammonium headgroup of ACh (Curtis et al., 1989; Kurtenbach et al., 1990; Spalding et al., 1994). However, Asp112^{3.32} is believed to participate in a hydrogen bond network with key residues near the top TMVII, a region that has been implicated previously in contributing to the binding pocket of prototypical modulators such as C₇/3-phth (Matsui et al., 1995; Voigtländer et al., 2003; Huang et al., 2005; Prilla et al., 2006; May et al., 2007a), and disruption of this network may account for the deleterious effects on C₇/3-phth binding.

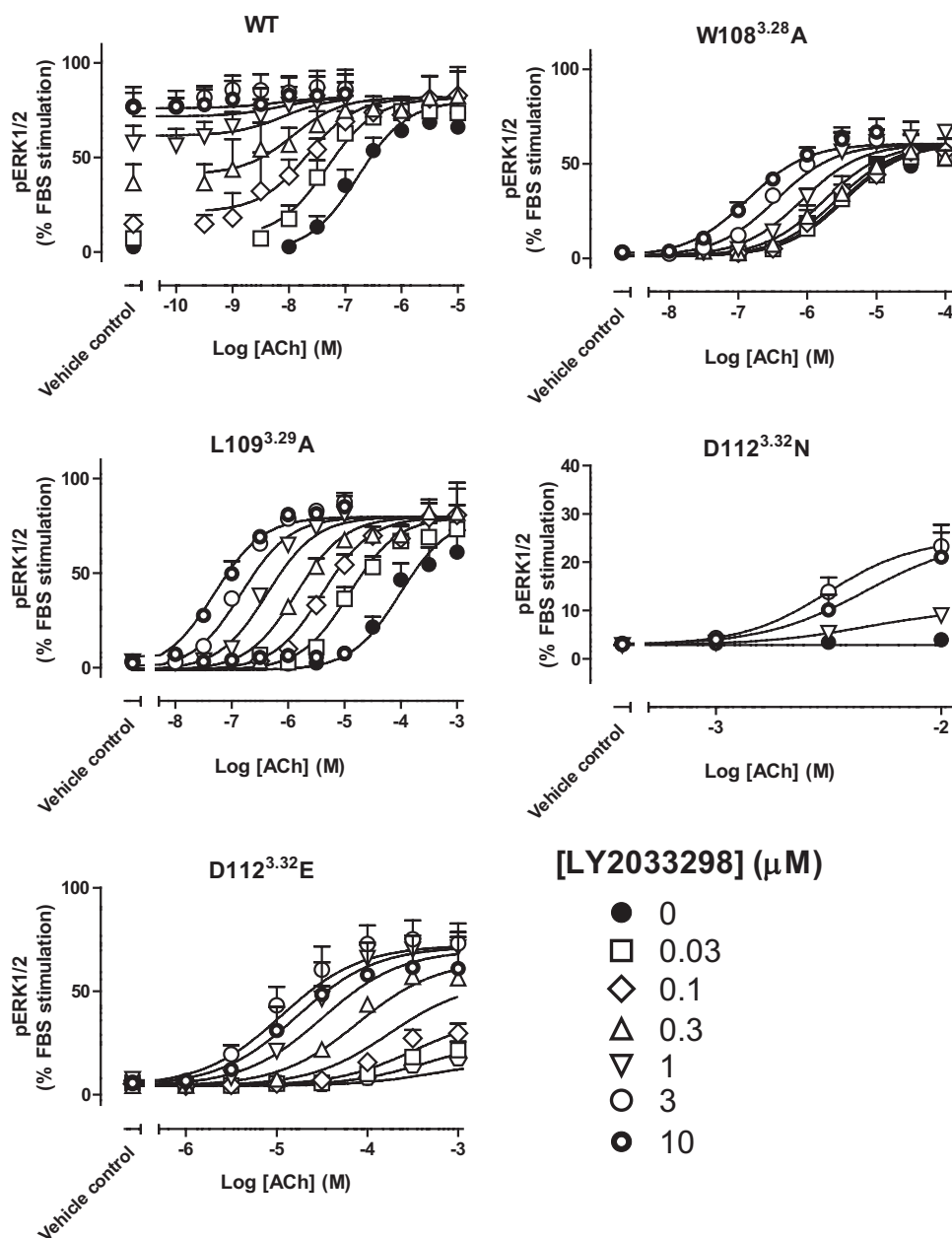


Fig. 7. LY2033298 rescues ACh efficacy at inactivating mutations. Peak levels of pERK1/2 were assessed as described under *Materials and Methods* and normalized to the response elicited by 10% FBS. The curves drawn through the points for data at the WT, Trp108^{3.28}, Leu109^{3.29}, and D112^{3.32}E constructs represent the best global fit of an operational model of allosterism (eq. 2) to each family of datasets, with the affinity of each agonist fixed to the pK_B value determined in separate binding assays (Table 1). Curves drawn through the points for data at the D112^{3.32}N construct represent the fit of each curve to a simple Hill equation. Data points represent the mean ± S.E.M. of at least three experiments performed in triplicate.

In contrast, the prototypical orthosteric ligands and atypical agonists used in this study were generally characterized by reduced binding affinity at a variety of the TMIII mutants with a few notable exceptions. The first was McN-A-343, which exhibited no significant difference in binding affinity at any mutant except the key D112^{3.32}N-M₄ mAChR construct. This finding is consistent with prior studies of the M₂ mAChR, in which McN-A-343 was unaffected by key orthosteric site mutations, in agreement with our hypothesis that this compound adopts a bitopic binding mode that extends up from Asp^{3.32} toward the extracellular loop regions (Valant et al., 2008; Gregory et al., 2010). The second exception was the modest increases in affinity noted for NDMC at the W108^{3.28}A mutant, for ACh and pilocarpine at the V120^{3.40}A mutant, and for ACh at the D129^{3.49}N mutant, respectively. The first of these observations is consistent with what has been noted for NDMC at the equivalent mutation introduced into the M₂ mAChR (Gregory et al., 2010) but is the opposite to the small decrease in its binding affinity at the equivalent mutation of the M₁ mAChR (Lebon et al., 2009), suggesting that NDMC adopts a slightly different binding pose at the even-numbered mAChRs compared with the M₁ mAChR.

It was also interesting to note that substitution of Ser116^{3.36} and Asn117^{3.37} to alanine caused a large reduction in the binding affinity of ACh but not in the affinity of any of the other ligands tested, indicating that ACh adopts a unique binding pose in comparison to the other agonists. It is unclear whether these residues are direct contact points for ACh, because although Ser116^{3.36} is predicted to face directly into the core of the orthosteric binding pocket (Han et al., 2005), Asn117^{3.37} is located below the predicted orthosteric binding site. Therefore, Asn117^{3.37} may serve to stabilize an important receptor conformation that is essential for ACh binding but not for any of the other ligands tested.

With regard to mutational effects on ligand signaling efficacy, it was of particular note that we did not identify any amino acids that were important for the functional activity of one particular class of agonist (orthosteric, allosteric, or atypical) to the exclusion of any others, suggesting that the location of the agonist binding site does not necessarily govern a unique activation mechanism after agonist binding and that there are some global receptor conformations that are favored by all agonists. Furthermore, with the exception of

ligand-specific effects of the V120^{3.40}A and D129^{3.49}N mutations, the rest of the mutations introduced into TMIII were generally deleterious to receptor activation. The substitution of Val120^{3.40} with alanine caused a significant increase in the signaling efficacy of pilocarpine, suggesting that even prototypical orthosteric ligands can sense different conformations compared with the endogenous ligand for the receptor. In contrast, the removal of the charge on Asp129^{3.49} caused an increase in the efficacy of all agonists tested, with the interesting exceptions of the endogenous orthosteric ligand ACh and the allosteric agonist LY2033298. The general view of mechanisms involving Asp^{3.49} in family A GPCR activation is that it forms an important hydrogen bond interaction with Arg^{3.50}, which itself interacts with Glu^{6.30} in the formation of a key “ionic lock”; disruption of this lock is proposed to be part of the activation mechanism for many GPCRs (Schwartz et al., 2006). This could explain why compounds such as pilocarpine, McN-A-343, and NDMC displayed enhanced signaling at this mutant receptor, assuming that the mutation placed the receptor in a partially active state with respect to ERK1/2 phosphorylation. However, prior studies at the M₁ and M₅ mAChRs have found minimal effects of the D^{3.49}N mutation on the efficacy of ACh itself (Lu et al., 1997; Burstein et al., 1998), which is also in agreement with our current study at the M₄ mAChR, suggesting that this mechanism need not be universal. It is noteworthy that the signaling efficacy of the allosteric agonist LY2033298 was also completely insensitive to the D^{3.49}N mutation. Overall, these findings are concordant with recent experiments on the β_2 adrenergic receptor, which showed that diverse agonists disrupt a different combination of molecular interactions responsible for stabilizing that receptor's inactive state (Yao et al., 2006).

Given that a key aim of our study was to also quantify the effects of TMIII mutations on the cooperativity between co-bound orthosteric and allosteric ligands on the M₄ mAChR, we reveal for the first time two key residues required for the transmission of binding cooperativity between LY2033298 and ACh. Trp108^{3.28} and Asp112^{3.32} were essential for the ability of LY2033298 to potentiate the binding affinity of ACh. Intriguingly, however, even though the binding cooperativity was almost abolished at the D112^{3.32}E mutant, the allosteric effect on signaling between ACh and LY2033298 was retained. In fact, at the L109^{3.29}A, D112^{3.32}E, and S116^{3.36}A mutants, an increase in efficacy modulation between LY2033298 and ACh was observed. This may be expected where ACh-mediated receptor signaling events are significantly impaired by an amino acid substitution if LY2033298 can restore them to functional receptors. It also highlights that an important yet often underappreciated mechanism of allosteric modulation is a “resetting” of energy barriers governing global transitions between receptor states by an allosteric modulator that subsequently facilitates (or hinders) the interaction with an orthosteric ligand.

In conclusion, the present study has identified conserved amino acid residues in the key TMIII domain that play a role in the binding, signaling and transmission of cooperativity in a diverse range of orthosteric, allosteric and atypical mAChR ligands. We have shown that although common activation switches are used by all classes of M₄ mAChR agonist, some subtle differences exist between the intramolecular interactions that are altered after the binding of different agonists.

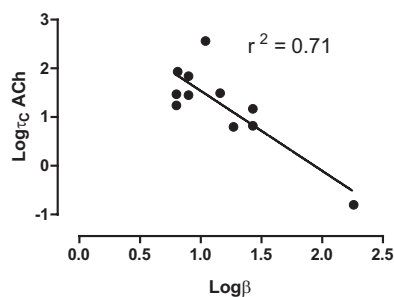


Fig. 8. The ability of LY2033298 to potentiate ACh activity correlates well with the efficacy of ACh at each mutant. ACh $\log\tau_c$ and $\log\beta$ values between ACh and LY2033298 were determined from fitting pERK1/2 interaction data at the WT and mutant receptors to an operational model of allosterism (eq. 2), as described under *Materials and Methods*. The line drawn through the points represents the best fit of a linear regression analysis to the data, where r^2 represents the correlation between $\log\tau_c$ and $\log\beta$.

Acknowledgments

We thank Dr. Celine Valant for the synthesis of C-/3-phth and Drs. Michael Crouch and Ron Osmond (TGR Biosciences) for the generous donation of AlphaScreen SureFire phospho-ERK1/2 reagents.

Authorship Contributions

Participated in research design: Leach, Davey, Sexton, and Christopoulos.

Conducted experiments: Leach and Davey.

Contributed new reagents or analytic tools: Felder.

Performed data analysis: Leach, Davey, and Christopoulos.

Wrote or contributed to the writing of the manuscript: Leach, Davey, Felder, Sexton, and Christopoulos.

Other: Christopoulos and Sexton acquired funding for the research.

References

- Altenbach C, Yang K, Farrens DL, Farahbakhsh ZT, Khorana HG, and Hubbell WL (1996) Structural features and light-dependent changes in the cytoplasmic inter-helical E-F loop region of rhodopsin: a site-directed spin-labeling study. *Biochemistry* **35**:12470–12478.
- Black JW and Leff P (1983) Operational models of pharmacological agonism. *Proc R Soc Lond B Biol Sci* **220**:141–162.
- Burstein ES, Spalding TA, and Brann MR (1998) The second intracellular loop of the m5 muscarinic receptor is the switch which enables G-protein coupling. *J Biol Chem* **273**:24322–24327.
- Chan WY, McKinzie DL, Bose S, Mitchell SN, Witkin JM, Thompson RC, Christopoulos A, Lazareno S, Birdsall NJ, Bymaster FP, et al. (2008) Allosteric modulation of the muscarinic M4 receptor as an approach to treating schizophrenia. *Proc Natl Acad Sci USA* **105**:10978–10983.
- Christopoulos A (1998) Assessing the distribution of parameters in models of ligand-receptor interaction: to log or not to log. *Trends Pharmacol Sci* **19**:351–357.
- Conn PJ, Jones CK, and Lindsley CW (2009) Subtype-selective allosteric modulators of muscarinic receptors for the treatment of CNS disorders. *Trends Pharmacol Sci* **30**:148–155.
- Curtis CA, Wheatley M, Bansal S, Birdsall NJ, Eveleigh P, Pedder EK, Poyner D, and Hulme EC (1989) Propylbenzylcholine mustard labels an acidic residue in transmembrane helix 3 of the muscarinic receptor. *J Biol Chem* **264**:489–495.
- Ehlert FJ (1988) Estimation of the affinities of allosteric ligands using radioligand binding and pharmacological null methods. *Mol Pharmacol* **33**:187–194.
- Elling CE, Thirstrup K, Holst B, and Schwartz TW (1999) Conversion of agonist site to metal-ion chelator site in the beta(2)-adrenergic receptor. *Proc Natl Acad Sci USA* **96**:12322–12327.
- Farrens DL, Altenbach C, Yang K, Hubbell WL, and Khorana HG (1996) Requirement of rigid-body motion of transmembrane helices for light activation of rhodopsin. *Science* **274**:768–770.
- Gether U, Lin S, Ghanouni P, Ballesteros JA, Weinstein H, and Kobilka BK (1997) Agonists induce conformational changes in transmembrane domains III and VI of the beta2 adrenoceptor. *EMBO J* **16**:6737–6747.
- Gregory KJ, Hall NE, Tobin AB, Sexton PM, and Christopoulos A (2010) Identification of orthosteric and allosteric site mutations in M2 muscarinic acetylcholine receptors that contribute to ligand-selective signaling bias. *J Biol Chem* **285**:7459–7474.
- Han SJ, Hamdan FF, Kim SK, Jacobson KA, Bloodworth LM, Li B, and Wess J (2005) Identification of an agonist-induced conformational change occurring adjacent to the ligand-binding pocket of the M(3) muscarinic acetylcholine receptor. *J Biol Chem* **280**:34849–34858.
- Hopkins AL and Groom CR (2002) The druggable genome. *Nat Rev Drug Discov* **1**:727–730.
- Huang XP, Prilla S, Mohr K, and Ellis J (2005) Critical amino acid residues of the common allosteric site on the M2 muscarinic acetylcholine receptor: more similarities than differences between the structurally divergent agents gallamine and bis(ammonio)alkane-type hexamethylene-bis-[dimethyl-(3-phthalimidopropyl)ammonium]dibromide. *Mol Pharmacol* **68**:769–778.
- Hubbell WL, Altenbach C, Hubbell CM, and Khorana HG (2003) Rhodopsin structure, dynamics, and activation: a perspective from crystallography, site-directed spin labeling, sulfhydryl reactivity, and disulfide cross-linking. *Adv Protein Chem* **63**:243–290.
- Hulme EC, Lu ZL, Bee M, Curtis CA, and Saldanha J (2001) The conformational switch in muscarinic acetylcholine receptors. *Life Sci* **68**:2495–2500.
- Hulme EC, Lu ZL, Saldanha JW, and Bee MS (2003) Structure and activation of muscarinic acetylcholine receptors. *Biochem Soc Trans* **31**:29–34.
- Jensen AD, Guarnieri F, Rasmussen SG, Asmar F, Ballesteros JA, and Gether U (2001) Agonist-induced conformational changes at the cytoplasmic side of transmembrane segment 6 in the beta 2 adrenergic receptor mapped by site-selective fluorescent labeling. *J Biol Chem* **276**:9279–9290.
- Jones CK, Brady AE, Davis AA, Xiang Z, Bubser M, Tantawy MN, Kane AS, Bridges TM, Kennedy JP, Bradley SR, et al. (2008) Novel selective allosteric activator of the M1 muscarinic acetylcholine receptor regulates amyloid processing and produces antipsychotic-like activity in rats. *J Neurosci* **28**:10422–10433.
- Kurtenbach E, Curtis CA, Pedder EK, Aitken A, Harris AC, and Hulme EC (1990) Muscarinic acetylcholine receptors. Peptide sequencing identifies residues involved in antagonist binding and disulfide bond formation. *J Biol Chem* **265**:13702–13708.
- Lazareno S and Birdsall NJ (1995) Detection, quantitation, and verification of allosteric interactions of agents with labeled and unlabeled ligands at G protein-coupled receptors: interactions of strychnine and acetylcholine at muscarinic receptors. *Mol Pharmacol* **48**:362–378.
- Leach K, Loiacono RE, Felder CC, McKinzie DL, Mogg A, Shaw DB, Sexton PM, and Christopoulos A (2010) Molecular mechanisms of action and in vivo validation of an M4 muscarinic acetylcholine receptor allosteric modulator with potential antipsychotic properties. *Neuropsychopharmacology* **35**:855–869.
- Leach K, Sexton PM, and Christopoulos A (2007) Allosteric GPCR modulators: taking advantage of permissive receptor pharmacology. *Trends Pharmacol Sci* **28**:382–389.
- Lebon G, Langmead CJ, Tehan BG, and Hulme EC (2009) Mutagenic mapping suggests a novel binding mode for selective agonists of M1 muscarinic acetylcholine receptors. *Mol Pharmacol* **75**:331–341.
- Lodowski DT, Angel TE, and Palczewski K (2009) Comparative analysis of GPCR crystal structures. *Photochem Photobiol* **85**:425–430.
- Lu ZL, Curtis CA, Jones PG, Pavia J, and Hulme EC (1997) The role of the aspartate-arginine-tyrosine triad in the m1 muscarinic receptor: mutations of aspartate 122 and tyrosine 124 decrease receptor expression but do not abolish signaling. *Mol Pharmacol* **51**:234–241.
- Matsui H, Lazareno S, and Birdsall NJ (1995) Probing of the location of the allosteric site on m1 muscarinic receptors by site-directed mutagenesis. *Mol Pharmacol* **47**:88–98.
- May LT, Avlani VA, Langmead CJ, Herdon HJ, Wood MD, Sexton PM, and Christopoulos A (2007a) Structure-function studies of allosteric agonism at M2 muscarinic acetylcholine receptors. *Mol Pharmacol* **72**:463–476.
- May LT, Leach K, Sexton PM, and Christopoulos A (2007b) Allosteric modulation of G protein-coupled receptors. *Annu Rev Pharmacol Toxicol* **47**:1–51.
- Motulsky H and Christopoulos A (2004) *Fitting Models to Biological Data Using Linear and Nonlinear Regression. A Practical Guide to Curve Fitting*. Oxford University Press, New York.
- Nawaratne V, Leach K, Felder CC, Sexton PM, and Christopoulos A (2010) Structural determinants of allosteric agonism and modulation at the M4 muscarinic acetylcholine receptor: identification of ligand-specific and global activation mechanisms. *J Biol Chem* **285**:19012–19021.
- Nawaratne V, Leach K, Suratman N, Loiacono RE, Felder CC, Armbruster BN, Roth BL, Sexton PM, and Christopoulos A (2008) New insights into the function of M4 muscarinic acetylcholine receptors gained using a novel allosteric modulator and a DREADD (designer receptor exclusively activated by a designer drug). *Mol Pharmacol* **74**:1119–1131.
- Prilla S, Schrobang J, Ellis J, Hölte HD, and Mohr K (2006) Allosteric interactions with muscarinic acetylcholine receptors: complex role of the conserved tryptophan M2422Trp in a critical cluster of amino acids for baseline affinity, subtype selectivity, and cooperativity. *Mol Pharmacol* **70**:181–193.
- Schwartz TW, Frimurer TM, Holst B, Rosenkilde MM, and Elling CE (2006) Molecular mechanism of 7TM receptor activation—a global toggle switch model. *Annu Rev Pharmacol Toxicol* **46**:481–519.
- Spalding TA, Birdsall NJ, Curtis CA, and Hulme EC (1994) Acetylcholine mustard labels the binding site aspartate in muscarinic acetylcholine receptors. *J Biol Chem* **269**:4092–4097.
- Sur C, Mallorga PJ, Wittmann M, Jacobson MA, Pascarella D, Williams JB, Brandish PE, Pettibone DJ, Scolnick EM, and Conn PJ (2003) N-desmethyloclozapine, an allosteric agonist at muscarinic 1 receptor, potentiates N-methyl-D-aspartate receptor activity. *Proc Natl Acad Sci USA* **100**:13674–13679.
- Valant C, Gregory KJ, Hall NE, Scammells PJ, Lew MJ, Sexton PM, and Christopoulos A (2008) A novel mechanism of G protein-coupled receptor functional selectivity. Muscarinic partial agonist McNA-343 as a bitopic orthosteric/allosteric ligand. *J Biol Chem* **283**:29312–29321.
- Voigtländer U, Jöhren K, Mohr M, Raasch A, Tränkle C, Buller S, Ellis J, Hölte HD, and Mohr K (2003) Allosteric site on muscarinic acetylcholine receptors: identification of two amino acids in the muscarinic M2 receptor that account entirely for the M2/M5 subtype selectivities of some structurally diverse allosteric ligands in N-methylscopolamine-occupied receptors. *Mol Pharmacol* **64**:21–31.
- Yao X, Parnot C, Deupi X, Ratnala VR, Swaminath G, Farrens D, and Kobilka B (2006) Coupling ligand structure to specific conformational switches in the beta2-adrenoceptor. *Nat Chem Biol* **2**:417–422.

Address correspondence to: Dr. Arthur Christopoulos, Drug Discovery Biology, Monash Institute of Pharmaceutical Sciences, Parkville, 3052, Victoria, Australia. E-mail: arthur.christopoulos@monash.edu